

# FINITE ELEMENT ANALYSIS OF LASER POWDER DEPOSITION OF TITANIUM

Paper 2005

Antonio Crespo, Augusto Deus, Rui Vilar

Dept. Materials Engineering and ICEMS, Instituto Superior Técnico, Av. Rovisco Pais 1, 1049-001 Lisboa, Portugal

## Abstract

A finite element thermo-kinetic model coupling heat transfer calculations with phase transformations kinetics was developed to simulate temperature field evolution and solid-state phase transformations during laser powder deposition of titanium. The model was used to study the influence of the deposition path geometry of single tracks on the melt pool stability and to estimate the adjustments of the deposition parameters necessary to avoid hot spots. This study was carried out by modelling the deposition of straight tracks as well as tracks with sharp and smooth corners. The addition of material was simulated by the activation of sets of elements that display curved cross and longitudinal sections, in order to describe the interaction zone.

## Introduction

Laser powder deposition (LPD) [1, 2] is a rapid manufacturing technique whereby 3D objects are fabricated by overlapping consecutive layers of laser melted material on top of previously resolidified ones. As each new layer is deposited, heat is conducted from the newly solidified material, through the previously deposited layers and into the substrate. The deposition of successive layers subjects the previously deposited material to consecutive thermal cycles that can induce phase transformations: the first cycle comprises the heating above melting temperature, followed by cooling down to a temperature in the solid-state region. The deposition step is followed by new heating-cooling cycles each time a subsequent layer of material is deposited. Ideally, previously deposited material should not be remelted during subsequent thermal cycles except for a thin surface layer, needed to ensure adhesion. The thermal cycles experienced by the material will differ from point to point and as a consequence, the phase constitution and properties of the material will vary from point to point too.

In a precedent publication it has been shown that the phase constitution and properties of steel parts manufactured by laser powder deposition can be predicted by means of a mathematical model that

couple heat transfer calculations with phase transformations kinetics information [3]. In the present paper, a finite element thermo-kinetic model for the laser powder deposition of titanium is described, which employs a similar methodology. However, whereas in the previous model material addition was simulated by activating parallelepipedic elements, in the present model a CAE (computer aided engineering) software was used to generate sets of elements with curved profiles which can be put together to form tracks of arbitrary shapes with curved cross sections and fronts.

The model was used to analyse heat transfer and phase transformations in single tracks of titanium with different geometries (straight lines and lines with a 90° corner, both sharp and smooth). While quasi steady state conditions remain for all geometries tested when deposition is performed on large substrates and away from edges, this is not the case when deposition is done on a small substrate or near the edges of the substrate, showing the usefulness of a modeling approach to adjusting the processing parameters in order to avoid hot spots which may generate defects or undesirable microstructures.

## Description of the model

Laser powder deposition of titanium was simulated by solving two sets of equations, one describing heat transfer and the other one the solid-state phase transformations kinetics in titanium induced by the changing temperature field. The complexity of the problem requires the use of numerical methods which involve discretization in both the space and time domains: the spatial problem is described by a mesh of points, where the heat transfer and phase transformations kinetics equations are solved in (ideally) infinitesimally small time steps. The deposition of material has to be accounted for by the introduction of new elements at the beginning of each step. The temperature field at each time step is calculated by the finite element method as a function of the material properties, part geometry and boundary conditions. Its evolution is used as input for a phase transformations kinetics subroutine which calculates

the evolution of the material's phase constitution due to the temperature variations experienced.

### Heat transfer analysis

The temperature on the workpiece is governed by the three dimensional heat conduction equation:

$$\rho c_p \frac{\partial T}{\partial t} = \nabla(k \cdot \Delta T), \quad (1)$$

where  $\rho$  is the density,  $c_p$  the specific heat and  $k$  the thermal conductivity of titanium, all temperature dependent. The heat input due to the laser radiation is described by a Gaussian surface heat flux:

$$Q_{laser}(x, y, t) = \alpha \frac{2P}{\pi r_l^2} \exp\left[-2\frac{r^2}{r_l^2}\right], \quad (2)$$

where  $\alpha$  is the absorption coefficient,  $P$  the laser beam power and  $r_l$  the laser beam radius. Heat losses due to convection (Eq. 3) and radiation (Eq. 4) are accounted for as terms of the boundary conditions:

$$Q_{convection} = h(T - T_0), \quad (3)$$

$$Q_{radiation} = \varepsilon \sigma (T^4 - T_0^4), \quad (4)$$

where  $T_0$  is room temperature,  $h$  the convective heat transfer coefficient,  $\varepsilon$  the emissivity and  $\sigma$  the Stefan-Boltzmann constant. The boundary condition takes the form:

$$k(\nabla T \cdot \vec{n}) = Q_{convection} + Q_{radiation} - Q_{laser}. \quad (5)$$

The heat transfer equation subjected to the above mentioned boundary conditions was solved using the finite element method. In this method the geometry of the part has to be represented by a mesh that reflects as closely as possible the geometry of the deposited track. To take into consideration material addition, the mesh must change at each time step by activating new elements which simulate the material deposited during the corresponding period of time. These elements are assumed to be at temperature  $T_{liquidus}$  at the moment of activation, in accordance with results of Neto and Vilar [4], who showed that the powder flying through the laser beam reaches liquidus temperature before impinging into the melt pool.

### Solid state phase transformations

During laser powder deposition the material is subjected to thermal cycles that vary from point to

point in the workpiece and induce phase transformations. For titanium these transformations are represented in the diagram of Figure 1.

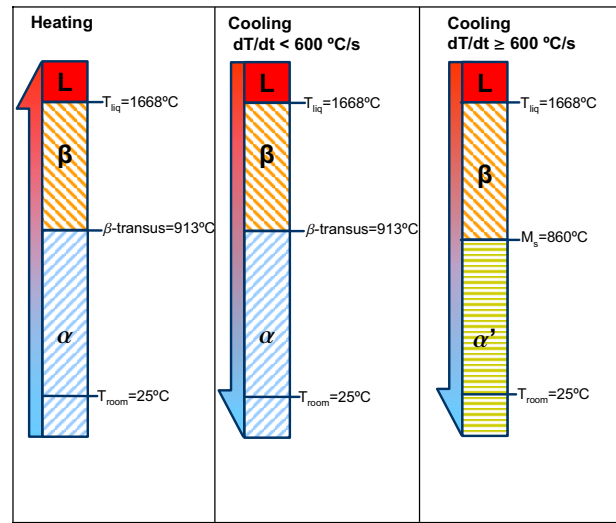


Figure 1 - Diagram of phase transformations in titanium.

Titanium presents an hexagonal close packed crystallographic structure ( $\alpha$  phase) at temperatures up to 913°C ( $\beta$ -transus temperature) and a body centred cubic structure ( $\beta$  phase) from 913°C to the melting temperature (1668°C) [5]. On cooling, the  $\beta$  phase formed by solidification will transform to  $\alpha$  at the  $\beta$ -transus temperature if the cooling rate is lower than a critical value of 600°C/s [6]. For larger cooling rates a martensitic transformation occurs, starting at 860°C ( $M_s$ ) and reaching completion at 810°C ( $M_f$ ), and  $\alpha'$  martensite is formed [6]. Due to the high cooling rates associated with laser processing the  $\beta$  phase usually transforms to martensite.

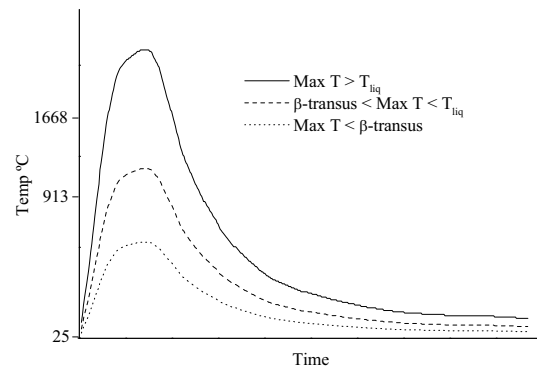


Figure 2 - Heating-cooling cycle for deposited material during deposition of a single track.

The sequence of phase transformations undergone by the material will depend on the maximum temperature reached during the experienced thermal cycles, which differs from point to point in the workpiece. When the maximum temperature exceeds the melting temperature this sequence will be  $\alpha \rightarrow \beta \rightarrow \text{Liquid} \rightarrow \beta \rightarrow \alpha'$ ; if the maximum temperature reached is between melting temperature and  $\beta$ -transus temperature  $\alpha \rightarrow \beta \rightarrow \alpha'$  will take place; no phase transformations occur when maximum temperature is below the  $\beta$ -transus (Figure 2).

### Track geometry

The sets of elements used in the model to simulate material addition (Figure 3) presented a curved cross section and a curved front, in agreement with experimental observations and previous models [7, 8]. These sets can be put together to form tracks of an arbitrary shape, as shown in Figure 4, that can be used to study the influence of the deposition path geometry in the temperature field.

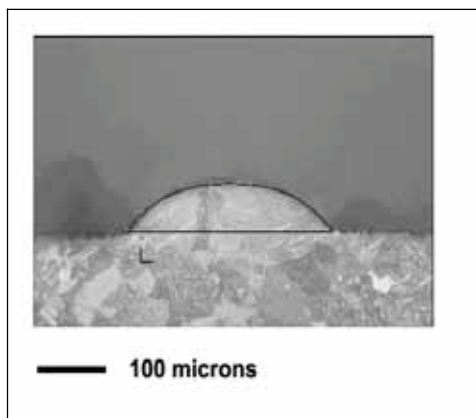
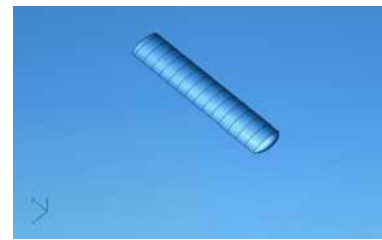


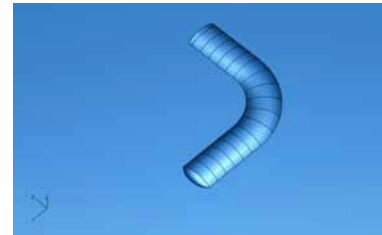
Figure 3 - Cross section of deposited tracks with superimposed track outline used in the model.

### Results

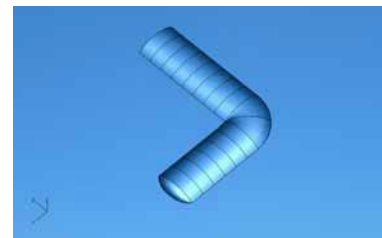
In the model heat transfer is assumed to occur only by conduction. To validate this assumption, the model prediction was compared with experimental results for the simpler case of laser melting. Laser melted tracks were prepared in titanium plates with laser beam powers ranging from 55W to 115W. Calculations were performed using the model without addition of material (Figure 5). The melt pool and the  $\beta$ -transformed region in the experimental samples were compared to those from the model (Figure 6 and Figure 7), showing a good agreement between experimental and modelling results.



4.a



4.b



4.c

Figure 4 - Tracks with different deposition paths: a - straight path; b - soft corner; c - sharp corner.

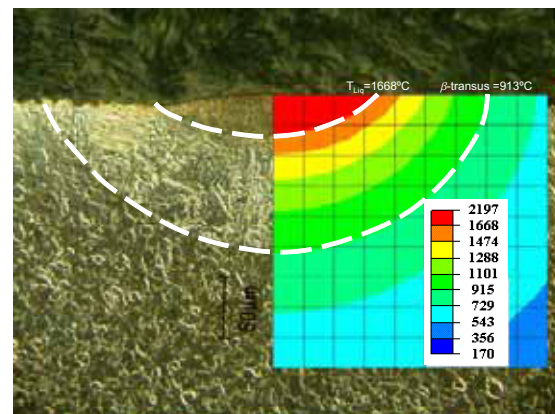


Figure 5 - Comparison of a laser melted sample with a model result showing the matching isotherms for the melting temperature and  $\beta$ -transus ( $P=75W$ ).

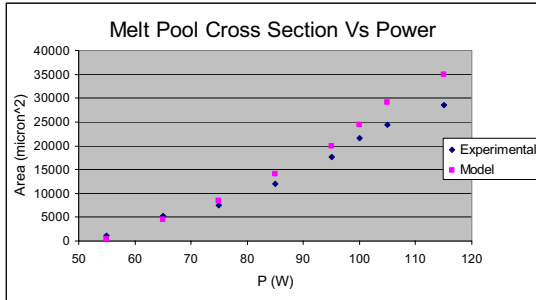


Figure 6 - Melt pool cross sectional area as a function of laser beam power.

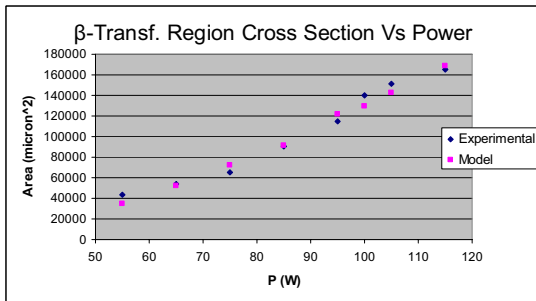


Figure 7 -  $\beta$ -transformed region cross sectional area as a function of laser beam power.

When large substrates are used and the deposition path is far away from edges, the simulation results for single track laser powder deposition show no noteworthy fluctuations of melt pool and heat affected zone dimensions for the different deposition paths tested, even when sharp corners were considered (Figure 8).

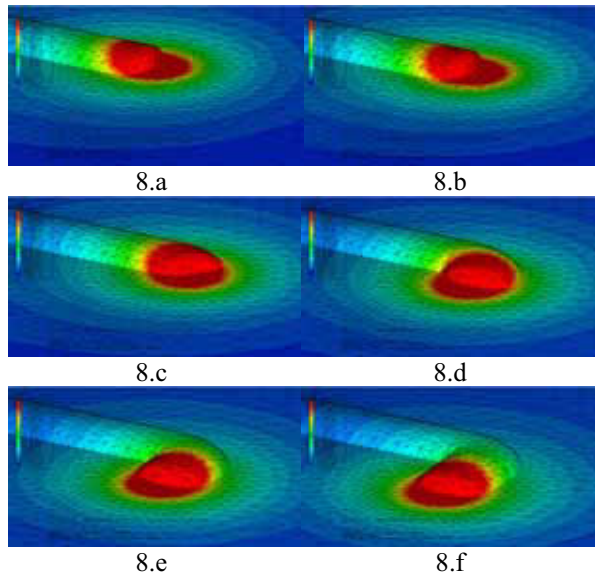


Figure 8 - Sequence showing a constant melt pool during deposition of a sharp corner (red - melt pool).

For smaller substrates or if deposition is performed near an edge of the substrate (Figure 9), heat accumulation occurs close to the edge, leading to an increase of the melt pool size. Heat accumulation gradually vanishes as the deposition path changes direction to the centre of the substrate (Figure 10).

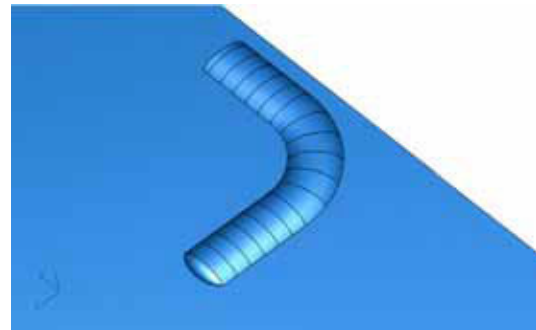
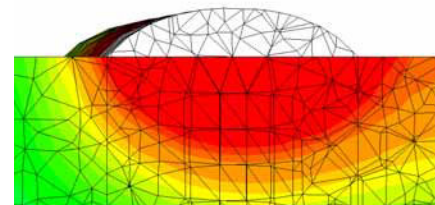
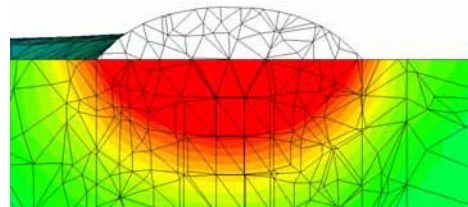


Figure 9 - Soft corner near the edge of the substrate.

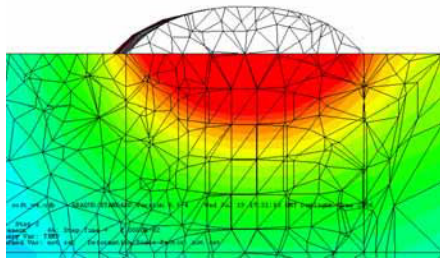


10.a

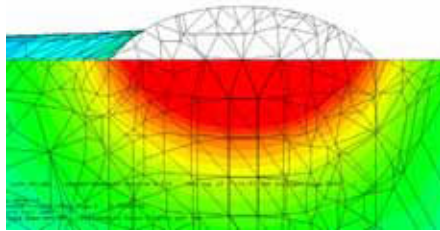


10.b

Figure 10 - Cross sections of the melt pool (in red); a - near the edge of the substrate; b - after the corner. Elements in white will be activated onto the melt pool and are shown for reference. Constant power 115W.



11.a

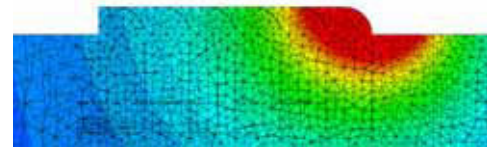


11.b

Figure 11 - Cross sections of the melt pool with power adjustment; a - near the edge of the substrate; b - after the corner. Power increase from 105W to 115W.

In order to keep constant melt pool shape and dimensions and to assure the stability of the process, the laser beam power must be varied so that power decreases in regions where heat accumulates, as near edges, and increases as the deposition path aims towards regions of the substrate where heat transfer away from the energy source is more efficient. Figure 11 shows cross sections of a track before and after a corner. The melt pool size was kept constant by decreasing the laser beam power to 105W just before the corner and continuously increasing it up to the nominal value of 115W after the corner.

The model was also used to predict the phase distribution during deposition and after cooling of the track down to room temperature. The results show that the phase distribution during deposition (Figure 12) consists of a melt pool surrounded by a region of  $\beta$  phase and a trailing region of  $\alpha'$ , which results from cooling the  $\beta$  phase below the  $M_f$  temperature. At room temperature, both the deposited material and the  $\beta$ -transformed region of the substrate consist of  $\alpha'$  (Figure 13).

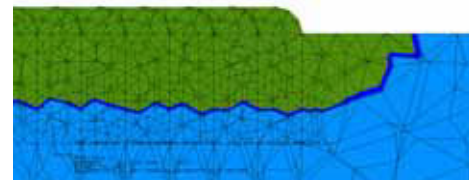


12.a

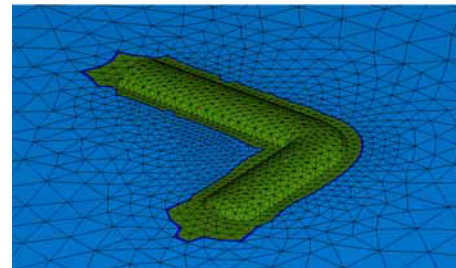


12.b

Figure 12 - Longitudinal section at an intermediary deposition step; a - temperature profile; b - phase profile (red - melt pool, blue -  $\alpha$ , green -  $\alpha'$ , orange -  $\beta$ ).



13.a



13.b

Figure 13 - Final phase composition; a - longitudinal section; b - overview (blue -  $\alpha$ , green -  $\alpha'$ ).

## Conclusions

A three-dimensional thermo-kinetic finite element model capable of simulating temperature and phase distributions during laser powder deposition of titanium has been developed. The model was applied to the deposition of single tracks with different geometries, including straight paths as well as smooth and sharp corners, in order to study the influence of the track geometry on the melt pool dimensions and the phase distribution. The results show that:

- the melt pool dimensions remain unchanged if the deposition is performed on large substrates and far away from the edges;
- if the deposition is performed on small substrates or near the edges, the laser beam power must be adjusted in order to prevent heat accumulation and formation of hot spots;
- the deposited material and the  $\beta$ -transformed region of the substrate undergo a martensitic transformation during cooling, therefore at the end of the deposition process these regions are composed of  $\alpha'$  martensite, while the composition of the rest of the substrate remains  $\alpha$  phase.

## References

- [1] R. Vilar (1999) Laser cladding, Journal of Laser Applications 2, 64-79.
- [2] L. Xue and M. U. Islam (2000) Free-form laser consolidation for producing metallurgically sound and functional components, Journal of Laser Applications 4, 160-165.
- [3] L. Costa, R. Vilar, T. Reti and A. M. Deus (2005) Rapid tooling by laser powder deposition: Process simulation using finite element analysis, Acta Materialia 14, 3987-3999.
- [4] O. O. D. Neto and R. Vilar (2002) Physical-computational model to describe the interaction between a laser beam and a powder jet in laser surface processing, Journal of Laser Applications 1, 46-51.
- [5] ASM International. Handbook Committee. (1990) ASM handbook, ASM International,

[6] S. K. Kim and J. K. Park (2002) In-situ measurement of continuous cooling  $\beta \rightarrow \alpha$  transformation behavior of CP-Ti, Metallurgical and Materials Transactions a-Physical Metallurgy and Materials Science 4, 1051-1056.

[7] A. F. A. Hoadley and M. Rappaz (1992) A Thermal-Model of Laser Cladding by Powder Injection, Metallurgical Transactions B-Process Metallurgy 5, 631-642.

[8] A. M. D. J. Mazumder (1996) Two-Dimensional Thermo-Mechanical Finite Element Model for Laser Cladding, in Proceedings of ICALEO '96, Orlando, FL, USA, 174-183

## Meet the Author(s)

Antonio Crespo is a researcher in the Laser Materials Processing Group of Instituto Superior Tecnico (IST), at Lisbon, Portugal, and is currently enrolled on his Ph.D.

Augusto Moita de Deus is a Professor in the Department of Materials Engineering of Instituto Superior Tecnico (IST), Lisbon, Portugal. He obtained his Ph.D from the Univ. Illinois at Urbana Champaign. At the present, he is working with the Materials Processing and Design Group of IST.

Rui Vilar is a Professor in the Department of Materials Engineering of Instituto Superior Técnico (IST), Lisbon, Portugal. He is the head of the Materials Processing and Design Group of IST.